Mantle flow pattern associated with the Patagonian slab window determined from azimuthal anisotropy

Walid Ben-Mansour (1, *), Douglas A. Wiens (1) , Hannah F. Mark (1, 2), Raymond M. Russo (3), Andreas Richter (4), Eric Marderwald (4) and Sergio Barrientos (5)

1 Department of Earth & Planetary Sciences, Washington University in Saint Louis, Saint Louis, MO, USA.

2 Woods Hole Oceanographic Institution, Woods Hole, MA, USA.

3 Department of Geological Sciences, University of Florida, FL, USA.

4 Laboratorio, MAGGIA, Universidad Nacional de La Plata, CONICET; La Plata, Argentina.

5 Centro Sismológico Nacional, Universidad de Chile, Santiago, Chile.

Corresponding author: walid.benmansour@seismo.wustl.edu

Key Points:

- Shear wave splitting indicates strong anisotropy with an E-W fast direction just south of the Chile Triple Junction and the edge of the subducting Nazca slab.
- The splitting and shear wave velocity structure suggest eastward shallow mantle flow in a 200-300 km wide channel around the edge of the Nazca slab.
- In most of southernmost Patagonia, splitting shows NE-SW fast directions consistent with large-scale asthenospheric flow.

****

Mantle flow pattern associated with the Patagonian slab window determined from azimuthal anisotropy

Walid Ben-Mansour [(1, *)], Douglas A. Wiens [(1)], Hannah F. Mark[(1, 2)], Raymond M. Russo[(3)], Andreas Richter[(4)], Eric Marderwald[(4)] and Sergio Barrientos[(5)]

1 Department of Earth & Planetary Sciences, Washington University in Saint Louis, Saint Louis, MO, USA

2 Woods Hole Oceanographic Institution, Woods Hole, MA, USA.

3 Department of Geological Sciences, University of Florida, FL, USA.

4 Laboratorio, MAGGIA, Universidad Nacional de La Plata, CONICET; La Plata, Argentina.

5 Centro Sismológico Nacional, Universidad de Chile, Santiago, Chile.

Corresponding author: Walid Ben-Mansour (walid.benmansour@seismo.wustl.edu)

Key Points:

- Shear wave splitting indicates strong anisotropy with an E-W fast direction just south of the Chile Triple Junction and the edge of the subducting Nazca slab.
- The splitting and shear wave velocity structure suggest eastward shallow mantle flow in a 200-300 km wide channel around the edge of the Nazca slab.
- In most of southernmost Patagonia, splitting shows NE-SW fast directions consistent with large-scale asthenospheric flow.

Abstract

Geological processes in Southern Patagonia are affected by the Patagonian slab window, formed by the subduction of the Chile Ridge and subsequent northward migration of the Chile Triple Junction. Using shear wave splitting analysis, we observe strong splitting of up to 2.5 s with an E-W fast direction just south of the triple junction and the edge of the subducting Nazca slab. This region of strong anisotropy is coincident with low uppermost mantle shear velocities and an absence of mantle lithosphere, indicating that the mantle flow occurs in a warm, low-viscosity, 200-300 km wide shallow mantle channel just to the south of the Nazca slab. The region of flow corresponds to a volcanic gap caused by depleted mantle compositions and absence of slab-derived water. In most of Patagonia to the south of this channel, splitting fast directions trend NE-SW consistent with large-scale asthenospheric flow.

Plain Language Summary

The subduction of the Chile Spreading Ridge beneath South America causes a gap in the subducting slabs beneath Patagonia, affecting locally the properties of the mantle. The deployment of new seismic instruments and available data allows us to study how the mantle seismic velocity varies with direction in the region. From the directional dependence of seismic velocity, we can infer the direction of mantle flow. A change from N-S to E-W mantle flow is observed in the Patagonian slab window. The flow occurs in a warm, low viscosity shallow mantle channel corresponding to a gap in activity along the volcanic arc.

1 Introduction

Slab windows, gaps between subducting slabs formed by the subduction of spreading ridges, offer an important opportunity to study the relationship between tectonic processes and mantle dynamics. They produce local thermal anomalies and have strong physical and chemical effects on the surrounding mantle. The slab window perturbs mantle flow associated with subduction of oceanic lithosphere, producing toroidal flow around the edges of subducted slabs [Peyton et al. 2001; Civello and Margheriti, 2004; Eakins et al. 2010; Russo et al., 2010a,b]. Such toroidal flow contributes to the thermal homogenization around the slab [Kincaid and Griffiths, 2004], and influences the temporal and spatial distribution of volcanism [Faccenna et al., 2010; Jadamec and Billen, 2010] and mantle mixing [Guillaume et al., 2010]. Slab windows provide an opportunity to study the strength and geographical pattern of toroidal flow at slab edges, as previously observed in the Mediterranean Sea [Civello and Margheriti, 2004] and the Western US [Zandt and Humphrey, 2008]. Recently, Mark et al. (2022) proposed a thermal and mechanical erosion process to explain slow mantle velocity anomalies and thinning of the lithospheric mantle between the Nazca slab edge and the northern part of the Patagonia slab window between 46˚ and 49˚S. This observation raises questions related to the 3-D shape and strength of toroidal flow around the slab edge which could contribute to thermo-mechanical erosion of the lithosphere, and the potential influence of mantle flow patterns on surface volcanism.

The Patagonia slab window is the best current example of a migrating slab window, formed as the Chile Triple Junction (CTJ) between the Nazca, South American, and Antarctic Plates moved from south to north beginning 16 m.y. ago [Breitsprecher and Thorkelson, 2009]. The CTJ has migrated ~1000 km northward, as ridge segments subparallel to the trench collided with the subduction margin [Breitsprecher and Thorkelson, 2009]. This evolution led to the formation of a gap in the subducting plate interface, allowing hot, buoyant, asthenospheric mantle to impinge on the South American plate from below, and producing mantle temperature and lithospheric thickness anomalies [Ávila and Dávila, 2018]. Arc volcanism and plate boundary seismicity occur along the cordillera, but south of the triple junction, the seismicity and the volcanism are sparser. Subduction of the Chile ridge segments 12 m.y. ago is thought to have caused a pronounced gap in the active Patagonian volcanic arc [Gutiérrez et al., 2005]. South of 53° latitude, the plate boundary between the South American plate and the Scotia plate is defined by the Magallanes-Fagnano Fault System,

77 a 600 km long continental transform fault with a slip rate of 0.7cm/yr [Roy et al., 2020]. The strike
78 of the fault system changes from NW-SE to EW around the longitude 68.5˚.
79
80 Early seismic studies have addressed the question of whether mantle flow between the Pacific and
81 Atlantic oceans was occurring beneath southern South America, through the Patagonian slab
82 window [Murdie and Russo, 1999; Helffrich et al, 2002; Russo et al. 2010a, b]. From body wave
83 tomography and shear wave splitting analysis, Russo et al. (2010a,b) show the presence of a slow
84 seismic velocity anomaly and large shear wave splitting times near the CTJ. They also show
85 variation in the fast direction of azimuthal anisotropy from ~N-S north of the triple junction to
86 ENE in the slab window. Beneath southernmost Patagonia (south of 51ºS), Helffrich et al. (2002)
87 show fast directions parallel to the absolute plate motion of the South American plate, interpreted
88 as the migration of material from the Pacific ocean to the Atlantic ocean.
89
90 From the analysis of short period group velocities derived from ambient noise cross-correlation,
91 Gallego et al. (2011) show the crust is affected by the slab window between 47ºS and 48ºS with
92 relatively low shear wave velocity in comparison with the average velocity and significant
93 anisotropy (1-2%). P-receiver function analyses [Rodriguez and Russo, 2020] show a crustal
94 thickness of 28-35 km proximal to the CTJ and thickening crust from 34 km just north of the triple
95 junction to ~55 km at 44ºS, with crustal thinning between 46.5ºS and 47ºS. In their joint inversion
96 of converted body wave phases and Rayleigh wave dispersion derived from ambient noise and
97 teleseismic earthquakes, Mark et al. (2022) show crustal thickening from south to north over the
98 slab window but also a thinning of the lithospheric mantle near the CTJ.
99
100 Here we present the results of a shear wave splitting analysis using SKS, SKKS and PKS phases
101 to characterize the mantle flow pattern beneath Southern Patagonia. We process broadband
102 seismograms from the recent GUANACO temporary deployment [Mark et al., 2022] as well as
103 previous deployments to measure shear-wave splitting parameters using the minimization of
104 transverse component energy method [Silver and Chan, 1991]. This new set of shear wave splitting
105 measurements provides an extended view of the large-scale azimuthal anisotropy in southern
106 South America and better constrains the mantle flow field associated with the Patagonia slab

window. We then discuss the source of anisotropy in the context of the slab window, regional structure, subduction dynamics, and mantle flow patterns in Southern Patagonia.

2 Datasets and analysis

2.1 Broadband seismic data

Much of the dataset comes from a recent deployment of the GUANACO (Glacial Uplift After Neoglaciation in the Andean Cordillera) temporary broadband network in Southern Patagonia. This network fills a data gap between the previous deployments in the CTJ region in the north [Russo et al. 2010a] and in southernmost Patagonia [Helffrich et al., 2002]. The GUANACO network was deployed from November 2018 to February 2021 and consisted of twenty-seven seismographs with station spacing of approximately 50 to 100 km [Mark et al., 2022]. The stations were equipped with Nanometrics Trillium-240 seismometers or Trillium Horizon sensors, and Quanterra Q330 dataloggers (see supplementary material). Additionally, we use all openly available broadband seismic data recorded in Southern Patagonia. These data come from Chilean broadband seismic networks (Chilean National Seismic Network, Red Sismológica Nacional); the 2004-2006 CRSP (Chile Ridge Subduction Project) [Russo et al., 2010a] and SEARCH (Seismic Experiment in the Aisen Region of Chile) datasets near the Chile Triple Junction; and the 1997-1999 SEPA (Seismic Experiment in Patagonia and Antarctica) deployment in Southernmost Patagonia [Helffrich et al., 2002]. All the stations used in the analysis are shown in Figure 1.

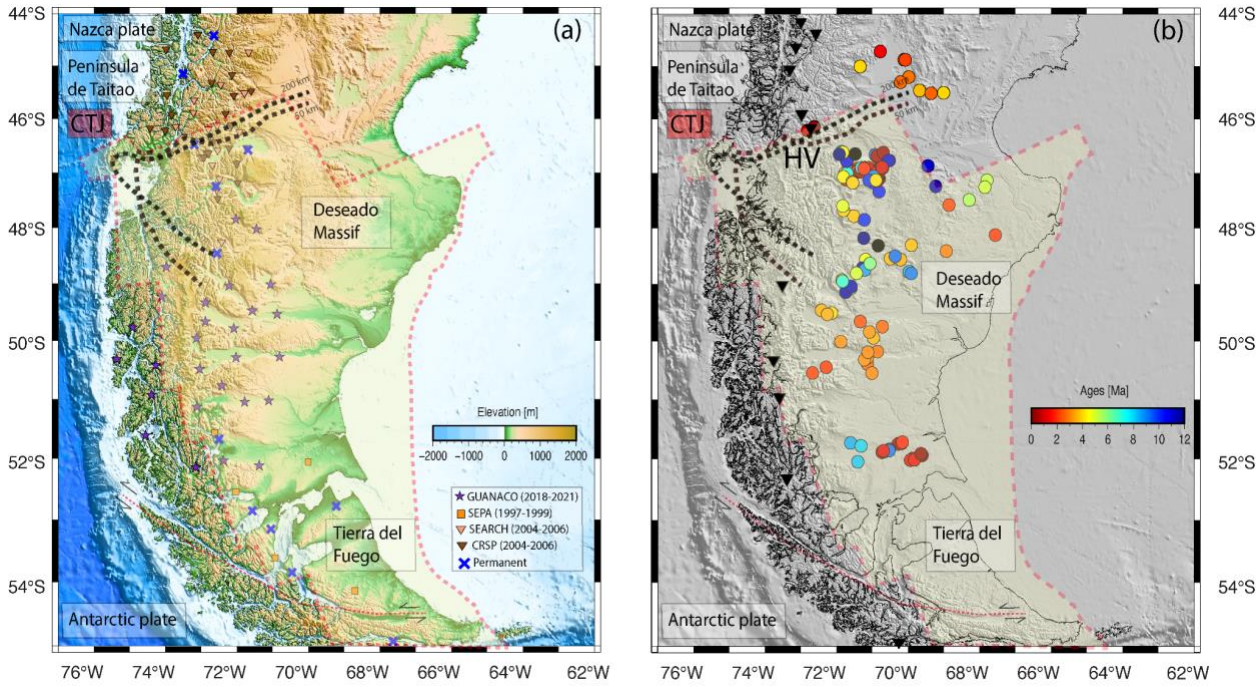

Figure1. (a) Topographic map of Southern Patagonia showing seismic stations used for this study. Yellow region shows the present-day extent of the slab window [Breitsprecher and Thorkelson, 2009]. The dashed lines represent the iso-depths (50 km in black and 200 km in red) defined by seismic velocity perturbation associated with the slab window [Russo et al., 2010a]. (b) Main tectonic features of the study region. Active arc volcanoes are shown by triangles. Ages of back-arc volcanism [compilation Guillaume et al., 2010] and mantle xenoliths [Melchiorre et al. 2020] are indicated by colored circles. *CTJ:Chile Triple Junction, HV:Hudson volcano.*

2.2 Shear wave splitting analysis

We perform shear wave splitting (SWS) measurements on all high quality SKS, SKKS, and PKS phases recorded at stations in the study area. We selected earthquakes of Mw ≥ 5.7 at epicentral distances of 87° to 140° from the study region for analysis. In the pre-processing, we apply different band-pass filters (6-50 s, 8-50 s, 10-50 s) to find the optimum frequency range and we use a signal-to-noise cutoff ratio of 2.0 for a given core-phase to reject bad or ambiguous signals. The final event sets used in this analysis come primarily from southeast Asia and the Alaska Aleutian subduction zones, with a few events from the Aegean-Anatolian regions.

We first estimate the single-phase splitting parameter for each event at each station by using the energy minimization method [Silver and Chan, 1991] using the SplitRacer code [Reiss and

Rumpker, 2017]. This approach determines the best splitting parameters (fast direction and delay time) that minimize the energy on the transverse component. For each event and each station, we assign a data quality (good-average-poor-null) based on different factors. A good signal to noise ratio for the phase we picked (SKS, SKKS or PKS) and a narrow uncertainty associated with the splitting parameters estimations from the grid search are deemed to be good splitting measurements. Splitting measurements with good signal to noise ratio but relatively large uncertainty deemed "average;" measurements showing no apparent splitting are referred to as "null". Null measurements most commonly arise when the fast or slow direction and the backazimuth of the event are very similar, so the shear wave is not split, and we cannot reduce the energy on the transverse component. We also deem measurements showing large uncertainties and small differences in the particle motion ellipticity pre and post rotation to be null. The choice of whether to assign a measurement to the "null" or "poor" categories depends on the signal-to-noise ratio and the ability to reduce the energy on the transverse component (see supplementary material).

To compute the average splitting parameters for a given station, we use the joint-splitting analysis method implemented in SplitRacer [Reiss and Rumpker, 2017]. This approach can reduce the influence of noise and provide a more robust measurement of the splitting beneath the station. In this approach, we apply the energy surface stacking method [Wolfe and Silver, 1998] to each phase (SKS-SKKS-PKS) and use only null and good split measurements from events recorded at a given station. As for the single-phase analysis, we use a grid search to find the best splitting operator that minimizes the energy of the stacked transverse components. We then classify the quality of the resulting joint splitting results, relying on the number of phases analyzed and the uncertainties of the derived splitting parameters to quantify the average splitting parameter measurements as good, average, or poor. Joint analyses with very few phases and/or large splitting parameter uncertainties are defined as "poor." Null measurements are also identified when the energy on the transverse component cannot be reduced. Poor and null measurements are not shown on maps or used in the interpretation.

In addition, we also estimate the splitting intensity, defined as the amplitude ratio between the transverse component energy and the time derivative of the radial component energy [Chevrot,

2000; Monteiller and Chevrot, 2010]. The results of the splitting intensity - where available - supplement the quality control of our splitting results.

3 Results

Results of individual and joint analysis of shear wave splitting parameters can be found in the Supplementary Materials. From more than 480 individual splits measurements, the final joint shear wave splitting parameters for individual stations comprise 33 good splits, 32 average splits and 16 null observations (Figure 2). Comparison of our measurements with previous analyses of open datasets for stations well north of the CTJ [Lynner and Beck, 2020] and south of our region under investigation in Tierra del Fuego [Helffrich et al., 2002] shows that we obtain similar results. Near the CTJ, our reprocessing of the CSRP network shows some differences with previous studies [Russo et al. 2010a]. These differences can be attributed mainly to different choices in the selection and processing of core phases. The shear wave splitting results (Figure 2a) show four different domains, from north to south: (1) a region with variable but approximately N-S fast directions and small average splitting times north of the triple junction; (2) a region with E-W fast directions and larger splitting times near the CTJ between 46.5˚S and 49˚S; (3) much of southernmost Patagonia, showing NE-SW fast directions and generally modest (< 1s) splitting times; and (4) a limited region with small delay times in Tierra del Fuego with E-W fast directions.

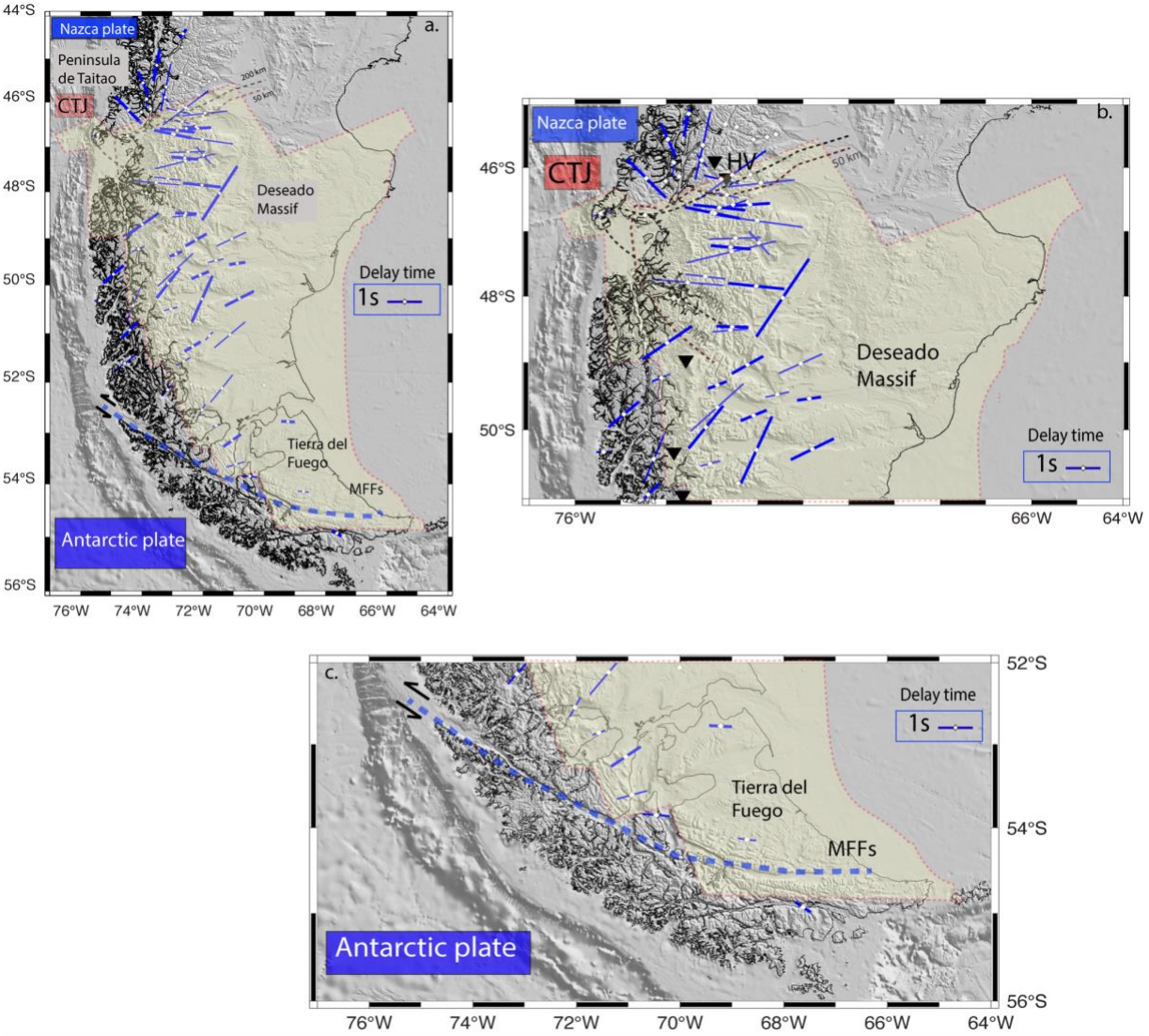

Figure 2. (a) Joint splitting results for the phases SKS-SKKS-PKS stacked at each station, assuming a single anisotropic layer. Thicker bars corresponding to good quality split measurements and thinner bars to average quality split measurements. (b) Zoom between 45˚S and 51˚S on the arc volcanism gap region and the edge of the Nazca slab (CTJ: Chilean Triple Junction; HV: Hudson Volcano). Active arc volcanoes are shown by triangles. (c) Zoom between 52˚S and 56˚S on the southernmost part of the continent (MFFs: Magallanes Fagnano Faults)

4 Discussion

4.1 Mechanism of anisotropy

Anisotropy inferred from SKS splitting is generally interpreted as the consequence of the lattice-preferred orientation (LPO) of olivine in the upper mantle, as the crust is typically too thin to

accumulate significant splitting [e.g., Savage, 1999]. However, both experimental geophysics and examination of mantle xenoliths show that olivine can form several different types of fabrics, making LPO interpretation more complex [Karato et al., 2008, and references therein]. Typically, in shear wave splitting studies, olivine A-type fabric, for which deformation aligns the crystallographic fast axis of olivine aggregates with the direction of maximum extension, is invoked, and observed fast splitting directions are assumed to parallel to horizontal mantle flow.

Differences in water content, pressure-temperature condition and stress regime will affect the olivine fabric types present within the mantle, producing fabrics different from the A-type described above. For example, D-type fabrics, appropriate for dry, high stress conditions, can occasionally be observed within the lithosphere. C and E -type fabrics are sometimes found in the asthenosphere, where significant water content and low stress conditions are expected [Karato et al., 2008]. However, these other fabrics result in shear wave splitting that is indistinguishable from A-type fabrics under horizontal flow conditions, and they are seldom invoked to explain teleseismic shear wave splitting measurements. One exception is B-type fabric, which is expected in regions with high water content and high stress [Karato et al., 2008], and has been used to explain trench-parallel shear wave splitting measurements in the supra-subduction mantle wedge regions of subduction zones [e.g., Long and Silver, 2008]. Conditions in the slab window are unlikely to be conducive to development of B-type olivine fabrics, however, as the absence of a dehydrating slab, relatively high temperatures due to asthenospheric inflow, and a relatively low stress regime except immediately adjacent to the lateral edge of the Nazca slab, are consistent with A-type or other fabrics with a fast direction in the flow direction [Jung et al., 2006]. Similar arguments apply to the asthenosphere throughout the region, which is likely to be too hot to allow B-type fabric to develop. The only exception is in the forearc, where lower temperatures and the presence of water may lead to B-type fabric [Karato et al., 2008]. Thus, we assume A-type, or fabrics that have a similar splitting relationship, in this discussion, with the possible exception of the forearc.

4.2 Toroidal flow in the uppermost mantle around the Nazca slab

Just to the south of the edge of the subducting Nazca slab, between 46˚S and 49˚S, we observe strong (delay times > 2 s) shear wave splitting with an E-W fast-axes orientation (Figures 2a-b). This direction contrasts with N-S fast axes orientations north of the CTJ, and with NE-SW fast

directions over most of the regions to the south which, as discussed below, likely reflects the average mantle flow direction in the region. We mapped larger splitting magnitudes (up to 2.5 s) in the area between 46˚S and 49˚S than elsewhere in the study region. The larger delay associated with the E-W fast direction compared to NE-SW fast directions elsewhere in Patagonia suggests vigorous mantle flow around the edge of the Nazca slab.

The anisotropy observations constrain the direction of maximum shear strain but leave an 180° ambiguity in the direction of mantle flow. Russo and Silver (1994) suggested that mantle flow from the Pacific to the Atlantic upper mantle occurred beneath the Nazca slab and then through slab gaps in the Caribbean and Scotia regions based on observations of trench parallel patterns in azimuthal anisotropy. Russo et al. [2010a, b] observed trench-parallel splitting fast directions north of the slab window, modulating into more E-W splitting directions in the slab window itself. They interpreted these results as due to flow beneath the Nazca slab turning through nearly 90º around the southern edge of the Nazca slab. This is consistent with recent modeling results suggesting mantle flow from the Pacific region to the Atlantic beneath Patagonia in the slab window region [Lin, 2014; Hu et al., 2017].

The region of inferred EW mantle flow around the Nazca slab coincides with a strong low velocity anomaly (Vsv < 4.1 km/s) in the uppermost mantle of the regional Vsv model [Mark et al., 2022]. The spatial distribution of E-W fast directions and low velocity uppermost mantle suggests the presence of a 200-300 km wide channel of vigorous flow at depths between 50 and 120 km (Figure 3). High velocity mantle lithosphere is completely absent, and low velocity mantle extends upward nearly to the crust. Since the mantle lithosphere is present both north and south of this region, this indicates that the mantle lithosphere has been thermally and mechanically eroded in the youngest part of the slab window. Energetic flow of warmer mantle immediately beneath the colder mantle lithosphere thermally perturbed and weakened the lithosphere, with some small pieces likely detaching and being carried eastward by the flow.

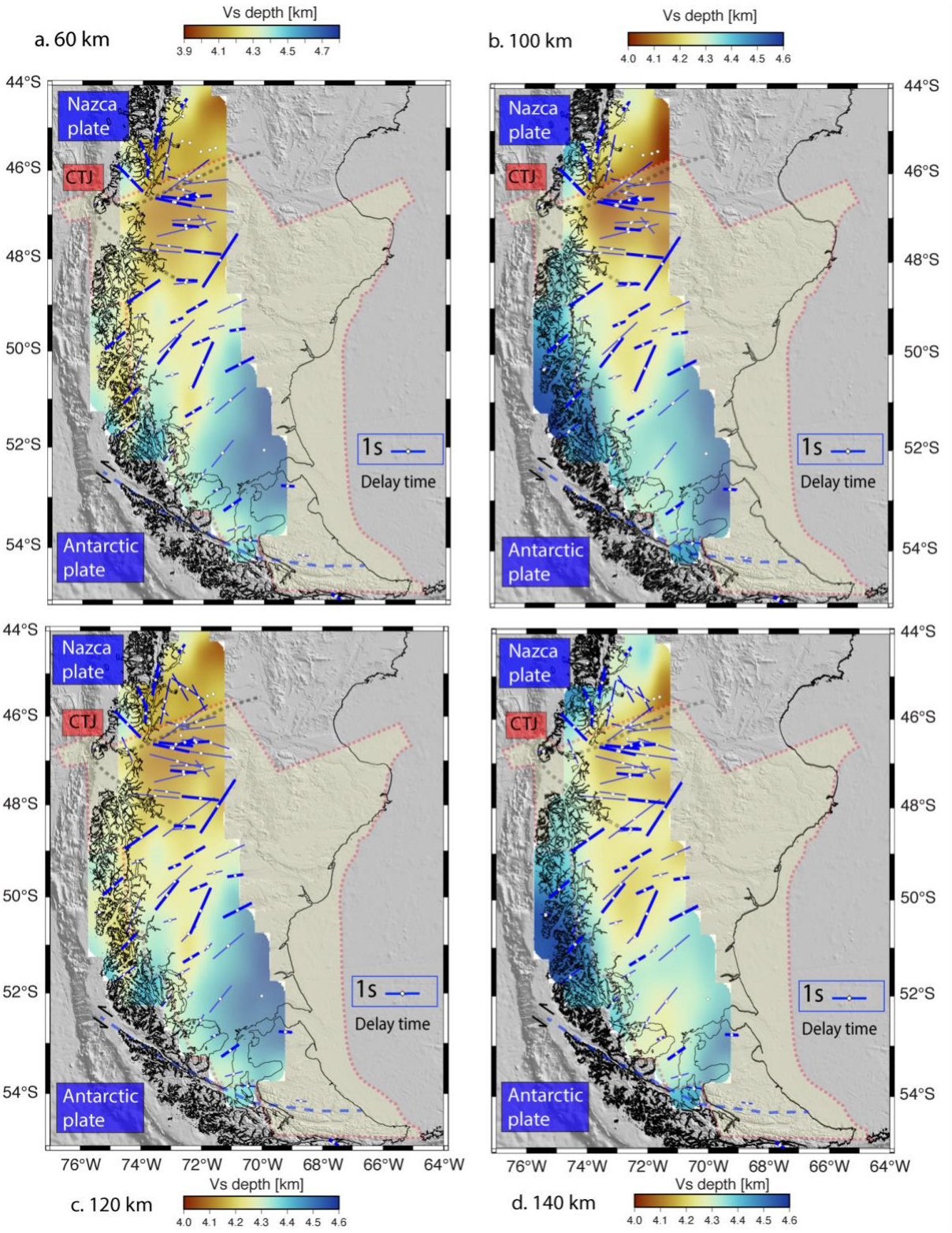

Figure 3. Comparison of the shear wave splitting results with the isotropic shear wave velocity model [Mark et al., 2022] at (a) 60 km, (b) 100 km, (c) 120 km and (d) 140 km depth. Thicker bars are good splitting measurements and thinner bars are average.

A ~300 km gap in the arc volcanism occurs in the same northern slab window region (Figure 1b) [Gutierrez et al. 2005]. Plate reconstructions [Breitsprecher and Thorkelson, 2009], tomographic imaging [Russo et al., 2010a], and intermediate-depth seismicity show that the northern edge of the volcanic gap corresponds to the southern edge of Nazca slab. The location of the slab gap corresponds closely with the extent of the slowest upper mantle velocities [Mark et al., 2022] and the large E-W oriented fast anisotropy directions (Figure 2a). Modeling studies show that slab edges are generally characterized by toroidal flow, and that complex and vigorous mantle flow can control the temperature distribution around the slab as well as the location of surface volcanism [Kincaid and Griffiths, 2004; Faccenna et al., 2010; Jadamec and Billen, 2010]. In the slab gap region, we are faced with an apparent discrepancy between vigorous mantle flow accompanied by very low upper mantle velocities, presumably reflecting elevated temperatures, and an absence of volcanism.

The most plausible explanation for the presence of the volcanic gap despite elevated mantle temperatures and vigorous mantle flow is the absence of slab-derived water necessary to generate melt at sub-arc conditions, as well as depleted upper mantle compositions. Most arc magmas are produced by flux melting, as fluids released from the slab infiltrate the mantle wedge and lower the solidus [Sobolev and Chaussidon, 1996; Grove et al., 2012]. In the absence of water from the slab, the upper mantle is likely similar to the mid-ocean ridge basalt (MORB) source region beneath the adjacent Chile Spreading Ridge, characterized by depleted compositions and low water contents. It is also likely that the vigorous west-to-east mantle flow in this region brings upper mantle material from beneath the Chile Spreading Ridge that has already undergone partial melting and extraction of water and incompatible elements, resulting in even stronger depletion in the slab gap. This results in a dry, depleted upper mantle incapable of melting even under the conditions of vigorous flow and elevated temperatures. There is petrological evidence for strong depletion in the slab gap area, as Hudson Volcano (Figure 1b), the volcano bordering the gap on the northern side, is interpreted as erupting a depleted MORB-type component derived from the Chile Spreading Center [Gutierrez et al, 2005].

4.3 Asthenospheric flow in Southernmost Patagonia

Shear wave splitting directions are largely NE-SW throughout the region south of 49°S. This direction of observed splitting is aligned with the azimuthal anisotropy directions of the global model SL2016svA at depths of 150-200 km over a large region of Southern South America and the South Atlantic [Schaeffer et al., 2016] (Figure 4), and we interpret this anisotropy as resulting from large-scale flow in the asthenosphere. This direction is also similar to the present-day flow velocities predicted for this region by a geodynamical model using a tomography-based buoyancy structure [Hu et al. 2017]. Asthenospheric anisotropy – rather than lithospheric anisotropy – probably dominates the shear wave splitting measurements from Southernmost Patagonia due to the large inherent strength of asthenospheric anisotropy at those depths [Debayle and Ricard, 2013]. The greater path length of the teleseismic shear waves in the asthenosphere relative to the mantle lithosphere, which is less than 100 km thick in this region [Mark et al, 2022], also implies an asthenospheric source for the observed splitting. Comparison with not-net rotation model [Argus et al., 2011] and hot spot reference model [Gripp and Gordon, 2002] suggest a decoupling between absolute plate motion and the azimuthal anisotropy pattern in this region (see supplementary material). Thus, the anisotropy reflects active asthenospheroc flow rather than passive shear deformation at the base of the lithospheric plates.

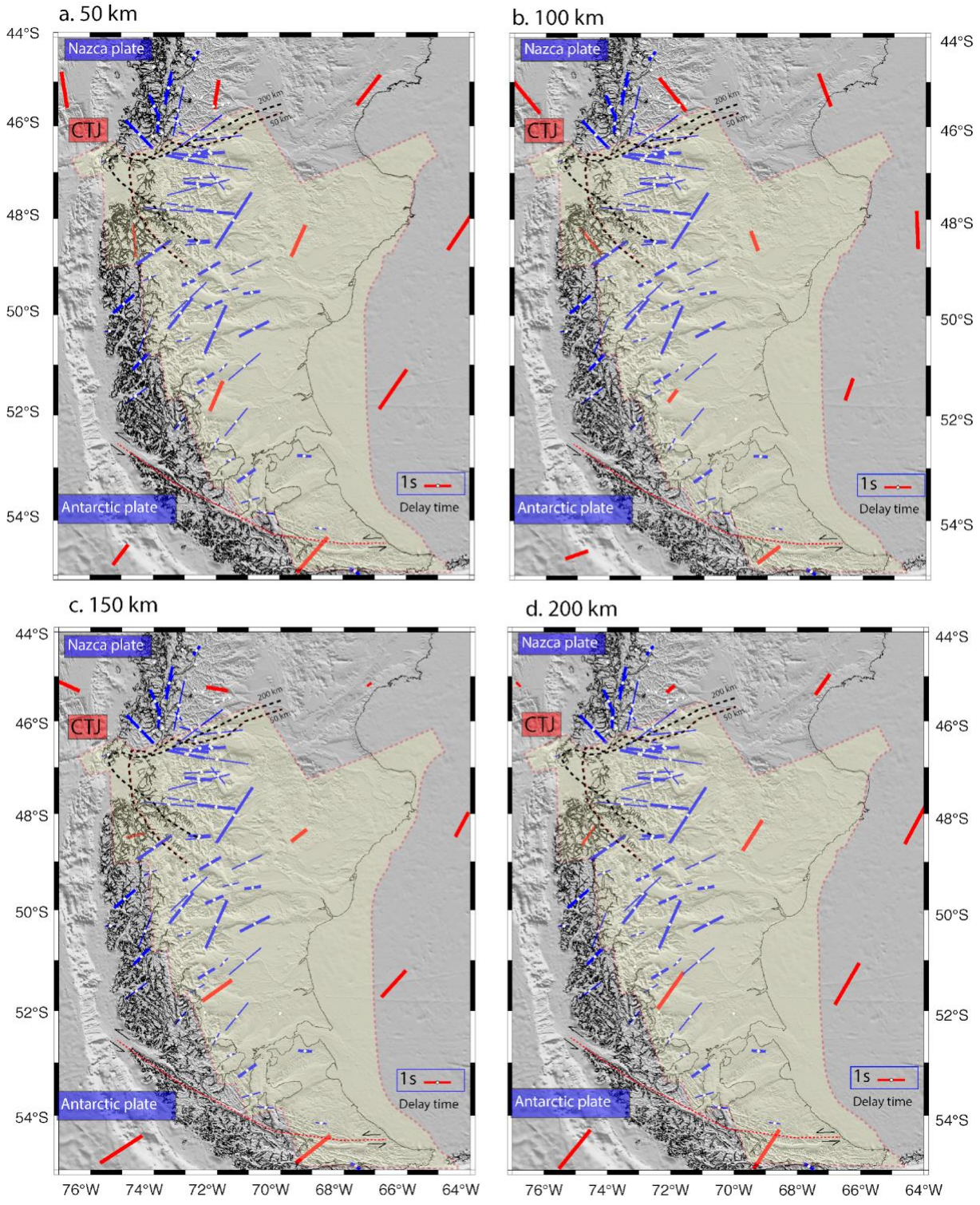

311

312 **Figure 4**. Comparison of shear wave splitting parameters (blue lines) with global azimuthal shear
313 velocity model SL2016svA [Schaeffer et al., 2016] at 50 km, 100 km, 150 km and 200 km (red
314 lines). Dashed red contour represents the slab window [Breistprecher and Thorkelson, 2009].

South of ~ 53.5° latitude, an E-W fast direction and smaller delay times (Figure 2c) suggest the presence of a different anisotropic domain relative to the NE-SW pattern observed from 49°-53°S. Fast direction measurements for stations near the Magallanes-Fagnano fault (MFFs) zone are parallel to the fault zone, the South America-Scotia plate boundary, with about 1 cm/yr of nearly E-W strike slip motion [Mendoza et al., 2022]. This observation suggests a potential relationship between the azimuthal anisotropy and this fault motion. Similar parallelism between azimuthal anisotropy has been observed at several other major strike-slip boundaries, such as the Alpine Fault in New Zealand [Zietlow et al., 2014]. Modeling of deformation along strike-slip shear zones suggests that lithospheric deformation and thus anisotropy will be more narrowly confined in the lithosphere but will broaden in the asthenosphere [Zietlow et al., 2014]. A denser distribution of stations would be required to constrain the depth and lateral distribution of the deformation in the fault zone.

5 Summary

The analysis of new data from seismic broadband instruments deployed in southern Patagonia between 2018 and 2021, along with open data from permanent stations and previous deployments, provides new constraints on the mantle flow pattern in this region. We develop a new shear wave splitting map for the region using energy minimization and joint analysis techniques. This map shows large splitting delay times and E-W fast directions just south of the southern edge of the Nazca plate between 46°S and 49°S, coinciding with a region of very low uppermost mantle shear velocities. We interpret this as indicating a vigorous toroidal flow pattern in the uppermost mantle around the edge of the Nazca slab. Low seismic velocities co-located with the E-W fast directions imply high mantle temperatures, suggesting the flow has thermally and mechanically eroded the mantle lithosphere. The region of vigorous flow corresponds to a volcanic gap caused by the depletion of mantle composition and an absence of water. A clear NE-SW fast direction from the shear wave splitting analysis in much of southernmost Patagonia reflects the regional asthenospheric flow. Near the Magallanes-Fagnano Fault accommodating South America-Scotia plate motion, splitting directions are E-W and parallel to the fault, consistent with deformation fabric produced by shear zones in the mantle beneath the fault.

Acknowledgments

We thank Celeste Bollini, Gerardo Connon, Leticia Duca, Nora Sabbione, Patrick Shore, Gerd Sielfeld, Daniel Valladares, Martin Vazquez, and many others for their work in planning, deploying, servicing, and recovering the GUANACO seismic array. Seismic instrumentation was provided by the Incorporated Research Institutions for Seismology (IRIS) through the PASSCAL Instrument Center at New Mexico Tech. Waveforms and metadata were accessed via the Incorporated Research Institutions for Seismology (IRIS) Data Management System. IRIS is funded by the Instrumentation and Facilities Program of the National Science Foundation. This research was funded by the National Science Foundation under grant EAR-1714154.

Open Research

Data used in this study is from the GUANACO, SEPA, SEARCH and CRSP temporary seismic networks (network codes: 1P, 10/2018-03/2021; XB, 02/1997-10/1998; XJ,12/2004-12/2006; YJ, 12/2004-12/2006), permanent stations from the Chile Network (network codes: C, C1). Data can be obtained from the IRIS DMC (https://ds.iris.edu/ds/nodes/dmc). Figures were produced using GMT software [Wessel et al. 2019]. Seismic stations information, and shear wave splitting results presented in this contribution can be found in the Zenodo repository 10.5281/zenodo.5655438.

References

Argus, DF, Gordon, RG, DeMets, C (2011). Geologically current motion of 56 plates relative to the no-net-rotation reference frame, *Geochemistry, Geophysics, Geosystems*,12,11.

Avila, P, Davila, FM (2018). Heat flow and lithospheric thickness analysis in the Patagonian asthenospheric windows, southern South America, *Tectonophysics*, 747,99-107.

Breitsprecher, Katrin and Thorkelson, Derek J (2009). Neogene kinematic history of Nazca--Antarctic--Phoenix slab windows beneath Patagonia and the Antarctic Peninsula, *Tectonophysics*,464,1--4,10--20.

Castellanos, J C, Clayton, RW, Perez-Campos, X. (2018). Imaging the eastern Trans-Mexican volcanic belt with ambient seismic noise: Evidence for a slab tear, *Journal of Geophysical Research: Solid Earth*,123,9, 7741--7759.

373 Chevrot, S. (2000). Multichannel analysis of shear wave splitting, *Journal of Geophysical*
374 *Research: Solid Earth*, 105, B9.
375 Civello, S, Margheriti, L (2004). Toroidal mantle flow around the Calabrian slab (Italy) from SKS
376 splitting, *Geophysical Research Letters*, 31,10.
377 Debayle, E, Ricard, Y (2013). Seismic observations of large-scale deformation at the bottom of
378 fast-moving plates, *Earth and Planetary Science Letters*, 376, 165--177.
379 DeMets, C, Gordon, RG, Argus, DF(2010). Geologically current plate motions, 181,1, 1--80.
380 Eakin, CM, Obrebski, M, Allen, RM, Boyarko, DC, Brudzinski, MR, Porritt, R. (2010). Seismic
381 anisotropy beneath Cascadia and the Mendocino triple junction: Interaction of the subducting slab
382 with mantle flow, *Earth and Planetary Science Letters*, 294, 3-4, 627--632.
383 Faccenna, C, Becker, TW, Lallemand, S, Lagabrielle, Y, Funiciello, F, Piromallo, C (2010).
384 Subduction-triggered magmatic pulses: A new class of plumes? *Earth and Planetary Science*
385 *Letters*, 299, 1-2. 54--68.
386 Gallego, A, Panning, MP, Russo, RM, Comte, D, Mocanu, VI, Murdie, RE, Vandecar, JC (2011).
387 Azimuthal anisotropy in the Chile Ridge subduction region retrieved from ambient noise,
388 *Lithosphere*, 3,6, 393--400.
389 Gripp, AE, Gordon, RG (2002). Young tracks of hotspots and current plate velocities, *Geophysical*
390 *Journal International*,150, 2 ,321--361.
391 Grove, TL, Till, CB, Krawczynski, MJ (2012), The role of H2O in subduction zone magmatism,
392 *Annual review of earth and planetary sciences*, 40,,413--439.
393 Guillaume, B, Moroni, M, Funiciello, F, Martinod, J, Faccenna, Claudio (2010). Mantle flow and
394 dynamic topography associated with slab window opening: Insights from laboratory models,
395 *Tectonophysics*, 496, 1-4, 83--98.
396 Gutierrez, F, Gioncada, A, Ferran, O G, Lahsen, A, Mazzuoli, R (2005). The Hudson Volcano and
397 surrounding monogenetic centres (Chilean Patagonia): an example of volcanism associated with
398 ridge-trench collision environment, *Journal of Volcanology and Geothermal Research*, 145,3-
399 4,207—233.
400 Helffrich, G, Wiens, D. A., Vera, E, Barrientos, S, Shore, P, Robertson, S, Adaros, R. (2002). A
401 teleseismic shear-wave splitting study to investigate mantle flow around South America and
402 implications for plate-driving forces, *Geophysical journal international*,149,1.

Helffrich, G (1995). Lithospheric deformation inferred from teleseismic shear wave splitting observations in the United Kingdom, *Journal of Geophysical Research: Solid Earth*, 100, B9, 18195--18204.

Hu, J, Faccenda, M, Liu, L (2017). Subduction-controlled mantle flow and seismic anisotropy in South America, *Earth and Planetary Science Letters*, 470,13--24.

Karato, SI, Jung, H, Katayama, I, Skemer, P (2008). Geodynamic significance of seismic anisotropy of the upper mantle: New insights from laboratory studies, *Annual review of earth and planetary sciences*, 36, 59--95.

Kincaid, C, Griffiths, RW (2004). Variability in flow and temperatures within mantle subduction zones, *Geochemistry, Geophysics, Geosystems*, 5, 6.

Jadamec, MA, Billen, Magali I (2010). Reconciling surface plate motions with rapid three-dimensional mantle flow around a slab edge, *Nature*, 465.

Jung, H, Katayama, I, Jiang, Z,Hiraga, T and Karato, S-I (2006). Effect of water and stress on the lattice-preferred orientation of olivine, *Tectonophysics*, 421,1--2,1--22.

Lin, SC (2014). Three-dimensional mantle circulations and lateral slab deformation in the southern Chilean subduction zone, *Journal of Geophysical Research: Solid Earth*,119 ,4, 3879--3896.

Long, MD, Silver, PG (2008). The subduction zone flow field from seismic anisotropy: A global view, *Science*, 319, 5861, 315--318.

Lynner, C, Beck, S L (2020). Subduction dynamics and structural controls on shear wave splitting along the South American convergent margin, *Journal of South American Earth Sciences* ,104.

Mark, HF, Wiens, DA, Ben Mansour, W., Ivins, E, Richter, A, Magnani, BM, Mardewald, E, Adaros, R, Barrientos, S. (2022). Thermal erosion of the lithosphere in the Patagonian slab window and implications for glacial isostatic adjustment, *Geophysical Research Letters*, 49.

Melchiorre, M, Faccini, B, Gregoire, M, Benoit, M, Casetta, F, Coltorti, M (2020). Melting and metasomatism/refertilisation processes in the Patagonian sub-continental lithospheric mantle: A review, *Lithos*, 354, 105324.

Mendoza, LPO, Richter, A, Marderwald, E R, Hormaechea, JL, Connon, G, Scheinert, M , Dietrich, R, Perdomo, R A (2022). Horizontal and vertical deformation rates linked to the Magallanes-Fagnano Fault, Tierra del Fuego: Reconciling geological and geodetic observations by modeling the current seismic cycle, *Tectonics*, 41, 1.

Monteiller, V, Chevrot, S (2010). How to make robust splitting measurements for single-station analysis and three-dimensional imaging of seismic anisotropy, *Geophysical Journal International*,182,1,311--328.

Murdie, RE, Styles, P, Prior, DJ, Daniel, AJ (2000). A new gravity map of southern Chile and its preliminary interpretation, *Revista geologica de Chile*, 27,1, 49--63.

Murdie, RE, Russo, RM (1999). Seismic anisotropy in the region of the Chile margin triple junction, *Journal of South American Earth Sciences*,12,3,261--270.

Ohtani, E (2020). The role of water in Earth's mantle, *National Science Review*,7,1, 224--232.

Peyton, V, Levin, V, Park, J, Brandon, M, Lees, J, Gordeev, E, Ozerov, A (2001). Mantle flow at a slab edge: Seismic anisotropy in the Kamchatka region, *Geophysical Research Letters*, 28, 2,379--382.

Ramos, VA (2005). Seismic ridge subduction and topography: Foreland deformation in the Patagonian Andes, *Tectonophysics*, 399,1-4, 73--86.

Reiss, MC, Rümpker, G (2017). SplitRacer: MATLAB code and GUI for semiautomated analysis and interpretation of teleseismic shear-wave splitting, *Seismological Research Letters*, 88, 2A, 392-409.

Rodriguez, EE, Russo, RM (2020). Southern Chile crustal structure from teleseismic receiver functions: Responses to ridge subduction and terrane assembly of Patagonia, *Geosphere*,16,1.

Roy, S, Vassallo, R, Martinod, J, Ghiglione, M, Sue, C, Allemand, P (2020). Co-seismic deformation and post-glacial slip rate along the Magallanes-Fagnano fault, Tierra Del Fuego, Argentina, *Terra Nova*, 321,1--10.

Russo, R M, Silver, P (1994). Trench parallel flow beneath the Nazca plate from seismic anisotropy, *Science*, 263, 5150, 1105-1111.

Russo, R M, VanDecar, J C, Comte, D, Mocanu, V I, Gallego, A, Murdie, R E. (2010a). Subduction of the Chile Ridge: Upper mantle structure and flow, *GSA Today*, 20, 9, 4-10.

Russo, R. M., Gallego, A., Comte, D., Mocanu,, V.I., Murdie, R. E., and VanDecar, J.C. (2010b). Source-side shear wave splitting and upper mantle flow in the Chile Ridge subduction region, *Geology*, 38, 707--710.

Savage, MK (1999). Seismic anisotropy and mantle deformation: what have we learned from shear wave splitting? *Reviews of Geophysics*, 37,1, 65--106.

Schaeffer, AJ, Lebedev, S and Becker, TW (2016). Azimuthal seismic anisotropy in the Earth's upper mantle and the thickness of tectonic plates, *Geophysical Supplements to the Monthly Notices of the Royal Astronomical Society*, 207,2, 901-933.

Silver, PG and Chan, WW (1991). Shear wave splitting and subcontinental mantle deformation, *Journal of Geophysical Research: Solid Earth*, 96, B10, 16429--16454.

Sobolev, AV, Chaussidon, M (1996). H2O concentrations in primary melts from supra-subduction zones and mid-ocean ridges: implications for H2O storage and recycling in the mantle, *Earth and Planetary Science Letters*,137,1-4,45—55.

Wessel, P, Luis, JF, Uieda, L, Scharroo, R, Wobbe, F, Smith, Walter HF, Tian, D (2019), The generic mapping tools version 6, *Geochemistry, Geophysics, Geosystems*,20,11, 5556--5564.

Wirth, E, Long, M D (2010). Frequency-dependent shear wave splitting beneath the Japan and Izu-Bonin subduction zones, *Physics of the Earth and Planetary Interiors*, 181, 3-4,141--154.

Wolfe, CJ, Silver, Paul G (1998). Seismic anisotropy of oceanic upper mantle: Shear wave splitting methodologies and observations, *Journal of Geophysical Research: Solid Earth*, 103, B1, 749--771.

Zandt, G, Humphreys, E (2008). Toroidal mantle flow through the western US slab window, *Geology*, 36,4 295—298.

Zietlow, DW, Sheehan, AF, Molnar, PH, Savage, MK, Hirth, G, Collins, JA, Hager, BH (2014). Upper mantle seismic anisotropy at a strike-slip boundary: South Island, New Zealand, *Journal of Geophysical Research: Solid Earth*, 119,2, 1020—1040.